Ultrasonic wireless sensor development for online fatigue crack detection and failure warning

Suyoung Yang[1], Jinhwan Jung[2], Peipei Liu[1], Hyung Jin Lim[1], Yung Yi[2], Hoon Sohn[*1] and In-hwan Bae[3]

[1]*Department of Civil and Environmental Engineering, Korea Advanced Institute of Science and Technology,*
291 Daehak-ro, Yuseong-gu, Daejeon, 34141, Korea
[2]*Department of Electrical Engineering, Korea Advanced Institute of Science and Technology,*
291 Daehak-ro, Yuseong-gu, Daejeon, 34141, Korea
[3]*New Airport Hiway Co., Ltd, 1048 Bongsudae-ro, Seo-gu, Incheon, 22694, Korea*

Abstract. This paper develops a wireless sensor for online fatigue crack detection and failure warning based on crack-induced nonlinear ultrasonic modulation. The wireless sensor consists of packaged piezoelectric (PZT) module, an excitation/sensing module, a data acquisition/processing module, a wireless communication module, and a power supply module. The packaged PZT and the excitation/sensing module generate ultrasonic waves on a structure and capture the response. Based on nonlinear ultrasonic modulation created by a crack, the data acquisition/processing module periodically performs fatigue crack diagnosis and provides failure warning if a component failure is imminent. The outcomes are transmitted to a base through the wireless communication module where two-levels duty cycling media access control (MAC) is implemented. The uniqueness of the paper lies in that 1) the proposed wireless sensor is developed specifically for online fatigue crack detection and failure warning, 2) failure warning as well as crack diagnosis are provided based on crack-induced nonlinear ultrasonic modulation, 3) event-driven operation of the sensor, considering rare extreme events such as earthquakes, is made possible with a power minimization strategy, and 4) the applicability of the wireless sensor to steel welded members is examined through field and laboratory tests. A fatigue crack on a steel welded specimen was successfully detected when the overall width of the crack was around 30 μm, and a failure warnings were provided when about 97.6% of the remaining useful fatigue lives were reached. Four wireless sensors were deployed on Yeongjong Grand Bridge in Souht Korea. The wireless sensor consumed 282.95 J for 3 weeks, and the processed results on the sensor were transmitted up to 20 m with over 90% success rate.

Keywords: wireless sensor; fatigue crack detection; nonlinear ultrasonic modulation; failure warning; steel structure; online monitoring

1. Introduction

A crack is one of the main causes for failures of metallic structures (Forrest 2013). In 1994, a single span of Seongsu Grand Bridge in South Korea suddenly fell down into a river due to a fatigue crack in a vertical flange. 32 people were killed and 17 people were injured by the downfall. In 2007, I-35W Highway Bridge in the United States of America collapsed due to a fatigue crack in a gusset plate, killing 13 people and injuring more than 100 people. As attested by these incidents, often fatigue cracks in metallic structures result in sudden failure of structures without proper warnings. Conventional low-frequency (below 100 Hz) vibration based techniques using accelerometers or dynamic strain gauges failed to detect incipient fatigue cracks with an overall width of 0.1 mm or less, and there is an increasing demand for estimating a remaining useful fatigue life in addition to crack diagnosis (Chan *et al.* 2004).

Acoustic emission (AE) (Roberts and Talebzadeh 2003, Mix 2005, Rabiei and Modarres 2013, Chen and Choi

2006), eddy current (EC) (Zilberstein *et al.* 2001, Knopp *et al.* 2009, Hamia *et al.* 2014), and ultrasonic techniques (Rokhlin and Kim 2003, Ihn and Chang 2004, Mi *et al.* 2006, Liu *et al.* 2014, Sohn *et al.* 2014, Lim *et al.* 2016) have been studied to detect fatigue cracks. Note that, even though there are also other nondestructive testing (NDT) techniques for crack detection such as magnetic particle, X-ray liquid penetrant tests, these techniques demand human intervention and are not suitable for online implementation.

The AE techniques detect fatigue cracks by sensing elastic stress waves released by crack initiation and propagation. Because the AE sensor used for elastic wave measurement should be always in an active mode, making the sensor very power hungry, and target signals are often buried under noisy environments, these techniques require sophisticated filters to discern damage signals from noise and may not be best suited for wireless online monitoring (Grosse *et al.* 2010, Nair and Cai 2010, Ruiz-Cárcel *et al.* 2014). The EC techniques identify cracks by detecting EC perturbation induced by fatigue cracks, and the EC techniques are sensitive to cracks. However, the lift-off distance between the EC sensor and the inspection surface needs to be maintained constantly and the sensing range of the EC sensor is only in the order of a few millimeters

---

*Corresponding author, Professor
 E-mail: sohnhoon@kaist.ac.kr

(Gholizadeh *et al.* 2015). The ultrasonic techniques have shown a promise for online implementation based on their high sensitivity to small cracks and large sensing range up to a few meters. Especially, nonlinear ultrasonic techniques are garnering popularity because of their superior sensitivity to fatigue cracks over conventional linear ultrasonic techniques (Sohn *et al.* 2014, Cantrell and Yost 2001, Zaitsev *et al.* 2006, Jhang 2009, Su *et al.* 2014). For example, the nonlinear ultrasonic modulation technique developed by Lim *et al.* detected a micro fatigue crack that is less than 100 μm wide (Lim *et al.* 2016). However, when it comes to wireless implementation, ultrasonic transducers are more power demanding than passive sensors such as strain gauges or accelerometers because additional power is required for ultrasonic wave generation as well as sensing.

In addition to fatigue crack detection, estimation of a remaining useful fatigue life is also an important issue. Several nonlinear ultrasonic techniques are developed for crack prognosis and failure prediction (Wu and Ni 2004, Sankararaman *et al.* 2011, Amura and Meo 2012, Fierro and Meo 2015, Nallasivam *et al.* 2008, Chen *et al.* 2016). These studies require additional information such as crack length measurements at multiple fatigue loading cycles and a prior knowledge of the specimen geometry for crack prognosis. Kim *et al.* developed an online structural failure warning system by discovering a relationship between structural failure and nonlinear ultrasonic modulation parameters without prior knowledge of the structure (Kim *et al.* 2018).

Conventional NDT, such as magnetic particle testing (MT), radiographic testing (RT), ultrasonic testing (UT), liquid penetrant testing (PT), and etc., and wire-based sensing are labor intensive and expensive (Tanner *et al.* 2003). This is because 1) only certified engineers can perform the NDT inspection, 2) special treatment of the target surface like grinding of the paints is necessary, and this preparation tends to be time consuming, and (3) many crack critical locations are hard to access, and additional inspection units like tower wagons are needed. On the other hand, wireless sensing is becoming popular for bridge health monitoring, because of their low installation and operation cost, ability to reach hard-to-access areas, etc. (Mainwaring *et al.* 2002, Sazonov *et al.* 2010). Many wireless sensors for vibration measurements (Lynch *et al.* 2006, Jang *et al.* 2010), crack detection (Caizzone *et al.* 2014, Liu *et al.* 2017), corrosion detection (Sunny *et al.* 2016, Zhang *et al.* 2016) and etc. have been developed and actually tested in real bridges. For online operation of wireless sensors, uninterrupted power supply and data transmission are very critical issues. To address the issues, a large volume of energy harvesting and wireless data transmission techniques have been reported (Jang *et al.* 2010, Chintalapudi *et al.* 2006, Wijetunge *et al.* 2010, Kilic 2014, Kwon *et al.* 2013, McCullagh *et al.* 2014, Marin *et al.* 2016).

This study develops a wireless sensor for online fatigue crack detection and failure warning based on measurement of crack-induced nonlinear ultrasonic modulation. The uniqueness of this study lies in that 1) a ultrasonic wireless sensor for online fatigue crack detection and failure warning is developed, 2) not only crack diagnosis but also failure
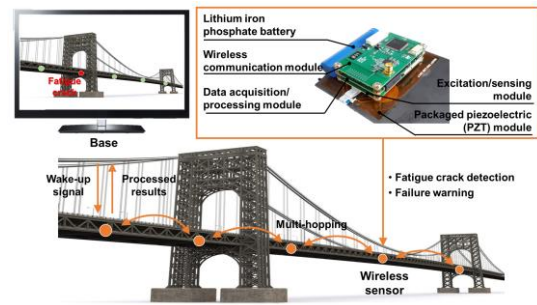

Fig. 1 Overview of the operation of the proposed wireless sensor

warning are given using crack-induced nonlinear ultrasonic modulation, 3) event-driven and power minimized operation of the wireless sensor is implemented so that the sensor can initiate inspection when extreme events such as earthquakes occur, and 4) the applicability of the wireless is validated through laboratory and field tests on steel welded members.

This paper is organized as follows. Section 2 provides an overview of the developed wireless sensor hardware. The proposed crack detection and failure warning algorithms are developed in Section 3. Then, Sections 4 and 5 present laboratory and field test results including a field test at Yeongjong Grand Bridge, respectively. Finally, a conclusion and discussions are provided in Section 6.

2. Development of a wireless sensor

2.1 Overview

As shown Fig. 1, the proposed wireless sensor is developed specifically for monitoring of metallic structures vulnerable to fatigue cracks. Ultrasonic waves are generated and measured using a packaged PZT module, an excitation/sensing module and a data acquisition/processing module in the wireless sensor. Then, the proposed monitoring algorithms in the data acquisition/processing module identify the presence of a fatigue crack and the imminent failure caused by the crack growth based on the measured nonlinear ultrasonic modulation responses. The wireless communication module in the wireless sensor is designed to operate in both periodic and event-driven modes. By default, the wireless sensor operates in the periodic mode. A base broadcasts a wake-up signal to wireless sensors with a pre-determined interval (three weeks) so that the wireless sensors periodically perform crack diagnosis, send out the outcomes, and go back to sleep. In the event-driven mode, the base sends out the wake-up signal to each wireless sensor right after the occurrence of an extreme event like an earthquake or typhoon. Then, the wireless sensor examines the assigned inspection area for crack formation and send back the crack diagnosis to the base.

2.2 Hardware development

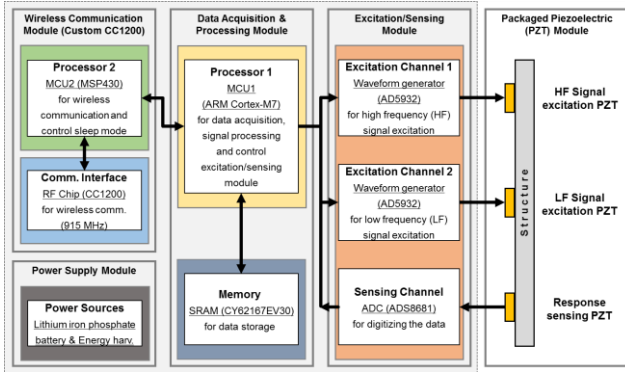The wireless sensor consists of five modules: packaged

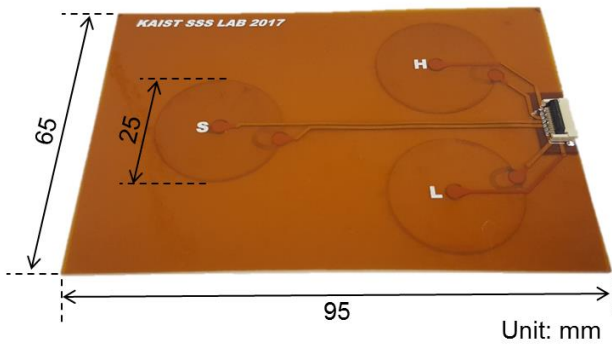Fig. 2 Five major modules of the proposed wireless sensor

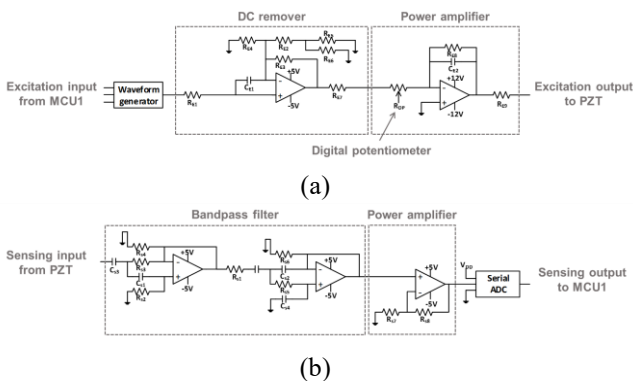Fig. 3 A prototype of the packaged PZT module

(a)

(b)

Fig. 4 Schematics of the excitation/sensing module: (a) excitation channel, and (b) sensing channel

PZT module, excitation/sensing module, data acquisition/processing module, wireless communication module and power supply module (Fig. 2).

As shown in Fig. 3, the packaged PZT module is composed of three identical PZT wafers with 25 mm diameter and 0.5 mm thickness (capacitance value of the PZT wafer is around 15 nF). Two PZTs are used for ultrasonic wave excitation, and the third one for sensing the corresponding response. The three PZTs are packaged by a Kapton tape with a printed circuit and connected to the excitation/sensing module through a flexible flat cable (FFC).

As shown in Fig. 4, there are two excitation channels and one sensing channel in the excitation/sensing module. Two sinusoidal inputs with different excitation frequencies are generated by the excitation channels, and the
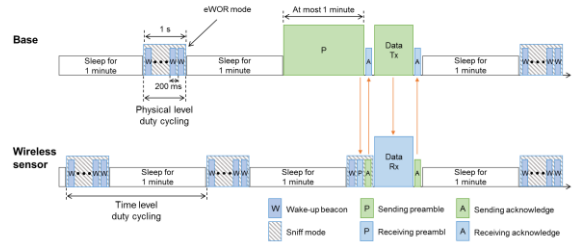

Fig. 5 The wireless communication protocol of the wireless sensor

corresponding response is measured by the sensing channel. Each excitation channel contains a waveform generator (Analog Device, AD5932), a direct current (DC) remover, a power amplifier, and a digital potentiometer. As shown in Fig. 4(a), the excitation channel can generate a signal with a peak-to-peak voltage of 24 V and a maximum frequency of 24 MHz. In this study, each excitation channel generates a sinusoidal input with a peak-to-peak voltage of 20 V and a frequency below 200 kHz. As shown in Fig. 4(b), the sensing channel consists of a bandpass filter, a power amplifier, and a 16-bit analog-to-digital converter (ADC) (Texas Instruments, ADS8681). High-frequency environmental and low-frequency structural vibration noises are removed by the second-order bandpass filter with a lower cutoff frequency of 2 kHz and a higher cutoff frequency of 500 kHz. The sampling rate of the ADC is 1 MHz, which is high enough to acquire the ultrasonic response generated by the excitation PZTs (typically below 200 kHz).

The digitized ultrasonic response is transmitted to the data acquisition/processing module through a serial peripheral interface (SPI). Because the MCU1 (micro controller unit, STMicroelectronics, ARM Cortex M7 32-bit STM32F765) in the data acquisition/processing module has a much faster clock speed (up to 216 MHz), MCU1 acquires the measured ultrasonic signals with little time delay (less than 5 μs). The measured data is first stored in a 256M-bit synchronous dynamic random access memory (SDRAM) (ISSI, IS42S32800J). Then, the data is brought back to the MCU1 and analyzed using the online fatigue crack detection and failure warning algorithms, which reside on the MCU1.

The wireless communication module consists of an MSP430 processor (MCU2) and a CC1200 radio-frequency (RF) chip (915 MHz IEEE 802.15.4 g transceiver). Since there are many obstacles inside bridge, the 915 MHz band is used for wireless communication than the conventional 2.4 GHz band. Initially, the wireless sensor is in a sleep mode for power conservation so that the excitation/sensing module and the data acquisition/processing module are turned off and only the MCU2 and the RF chip in the RF communication module operate in their low power modes (MCU2: standby mode (LPM3), RF chip: power down mode). The mode of the RF chip mode is switched to a sniff mode once every minute so that the wake-up signal from a base, if any, can be recognized by the wireless communication module. In the sniff mode, the MCU2 is still in its low power mode and the RF chip is in an

enhanced wake-on-radio (eWOR) mode to receive the wake-up signal. Once the wake-up signal is received, MCU2 wakes up MCU1 in the data acquisition/processing module and the data acquisition and processing module initiates ultrasonic measurement through the excitation/sensing module (active mode). The diagnosis is transmitted to the base through multi-hopping.

The wireless communication protocol between the wireless sensor and the base follows two-levels duty cycling MAC, which consists of time level duty cycling and physical level duty cycling. By the two-levels duty cycling MAC, the wireless sensor can operate in the periodic mode without time synchronization and also in the event-driven mode for rare extreme events like earthquakes. As shown in Fig. 5, whenever the pre-determined interval (3 weeks) is reached or some extreme events such as earthquakes occur, the base transmits a preamble (wake-up signal) for at most one minute until the wireless sensor receives the preamble in its sniff mode. Once the wireless sensor receives the preamble, the wireless sensor sends an acknowledge to the base. Then, data transmission is initiated, and the wireless sensor sends another acknowledge to the base again to report the reception of the data. The base and the wireless sensor are in the sniff mode every one minute (time level duty cycling), and the wake-up beacon is sent around every 200 ms in the sniff mode (physical level duty cycling). Unlike other techniques that continuously send the wake-up beacon, the physical level duty cycling can save the energy consumed in the sniff mode by sending the wake-up beacon with a shorter interval.

One lithium iron phosphate battery (ENIX Energies, 18650) with 3.2 V nominal voltage and 1500 mAh capacity furnishes a stable power to the wireless sensor. Solar and vibration energy harvesting techniques are also applied to charge the battery of the wireless sensor (Sohn *et al.* 2016, Yang *et al.* 2018). To minimize the power consumption of the wireless sensor, metal-oxide-semiconductor-field-effect transistor (MOSFET) relays (OMRON, G3VM-21HR), which can support continuous current up to 2.5 A, are employed in the excitation/sensing module and the data acquisition/processing module. In the sleep mode of the wireless sensor, the MCU2 turns off the MOSFET relay in the data acquisition/processing module. In this way, the excitation/sensing module and the data acquisition/processing module do not consume any power when the wireless sensor is in its sleep mode. The energy consumption of the wireless sensor for the duty cycle of three weeks is 282.95 J, and it is estimated that the battery can operate the wireless sensor for 1.5 years.

3. Development of fatigue crack detection and failure warning algorithms

3.1 Overview of nonlinear ultrasonic modulation

The amplitude modulation between a high frequency (HF) ultrasonic input and a low frequency (LF) ultrasonic input generates nonlinear ultrasonic modulation (Van Den Abeele *et al.* 2000). If two ultrasonic waves at two different frequencies ω_a (LF) and ω_b (HF) were created to a linear (intact) structure, the responses only at the two input frequencies would appear in the frequency domain. If the structure had a crack, the ultrasonic response would appear not only at the input frequencies but also at their harmonics (multiples of input frequencies) and modulations (linear combinations of input frequencies) generated by crack opening and closing (De Lima and Hamilton 2003, Duffour *et al.* 2006). In this study, the phenomenon of nonlinear ultrasonic modulation is utilized for fatigue crack detection. Note that the nonlinear ultrasonic modulation occurs only when the following binding conditions are satisfied (Lim *et al.* 2014): (1) Crack perturbation: both of two inputs should oscillate the strain (displacement) at the crack location. In vibrations, the crack perturbation condition means that nonlinear ultrasonic modulation components do not occur at the nodes of the vibration modes, (2) Mode matching: The generation of the nonlinear ultrasonic modulation depends on the selection of two input frequencies. The binding conditions can also be affected by crack configurations and environmental and operating conditions of the structure, thus application of multiple combinations of HF and LF inputs will be desirable for field applications. Furthermore, nonlinear responses can also be generated due to atomic nonlinearity and/or material nonlinearity. However, their amplitudes are often much smaller than those produced by crack formation (Liu *et al.* 2017).

3.2 Autonomous fatigue crack detection algorithm

First, both HF and LF inputs are simultaneously excited to the structure, and the response $u_{\omega_b \pm \omega_a}$ at the first sideband frequencies ($\omega_b \pm \omega_a$) are acquired by a discrete Fourier transform (DFT). Second, the HF input alone is applied to the structure N times, and the responses at the first sideband frequencies ($n_{\omega_b \pm \omega_a, i}, i = 1, 2, \ldots, N$) are obtained. Note that, because only the HF input is applied here, the response at the first sideband frequencies are only noises. Then, an exponential distribution is fitted to the population of $n_{\omega_b \pm \omega_a, i}$, and a threshold $T_{\omega_b \pm \omega_a}$ corresponding to a user specified one-sided confidence interval is established. Finally, the nonlinear indices NI at the first sideband frequencies are defined as

$$\text{NI}_{\omega_b \pm \omega_a} = u_{\omega_b \pm \omega_a} - T_{\omega_b \pm \omega_a} \tag{1}$$

The nonlinear index shows how large the nonlinear modulation response, $u_{\omega_b \pm \omega_a}$, is compared to the inherent noise level, $T_{\omega_b \pm \omega_a}$. Therefore, the NI values tend to be negative for an intact case. For a damage case with a fatigue crack, the NI values increase and become positive. By computing the skewness and median statistics of the NI values obtained from various combinations of input HF and LF frequencies, the presence of a fatigue crack is determined as follows (Lim *et al.* 2016).

If both skewness and median values of the NI values are negative, the structure is intact. Otherwise, the structure has a fatigue crack.

Here, the skewness and median statistics are complementary to each other. When only a few frequency combinations among all the frequency combinations satisfy the binding conditions, the skewness statistics is more

sensitive to fatigue crack formation. When the majority of frequency combinations meet the binding conditions, the median statistics becomes more effective in detecting a fatigue crack.

3.3 Autonomous failure warning algorithm

The nonlinear ultrasonic modulation parameter β is defined as follows

$$\beta = \frac{4(u_{\omega_b+\omega_a}+u_{\omega_b-\omega_a})}{u_{\omega_a}u_{\omega_b}\kappa_a\kappa_b} \tag{2}$$

where κ_a and κ_b are the wavenumbers of the responses at ω_a and ω_b, respectively (Fierro and Meo 2015). When one of u_{ω_a} or u_{ω_b} values in Eq. (2) is close to zero, the β value becomes infinite. To avoid this problem, an average nonlinear parameter β_{avg} is introduced by considering all the input frequency combinations

$$\beta_{avg} = \frac{1}{n}\sum_{i=1}^{n}\beta_i = \frac{1}{n}\frac{\sum(u_{\omega_b+\omega_a,i}+u_{\omega_b-\omega_a,i})}{\sum u_{\omega_a,i}\sum u_{\omega_b,i}} \tag{3}$$

where n is a total number of the input frequency combinations, and the subscript i denotes the value acquired from the ith input frequency combination.

As a fatigue crack grows, the β_{avg} value initially increases (Amura and Meo 2012, Li *et al.* 2016). Once the crack length reaches a certain level, the crack starts to grow rapidly following a fracture mechanism, rather than a fatigue mechanism. At this transition point, the β_{avg} value suddenly drops because the crack opening and closing become weak as the crack becomes large. Hence, a failure warning can be provided when a sudden decrease of β_{avg} (Indicator II) occurs after a rapid increase of β_{avg} (Indicator I) (Kim *et al.* 2018).

The autonomous fatigue crack detection and failure warning algorithms described here are implemented using C# programming language and uploaded on MCU1 in the data acquisition/processing module.

4. Laboratory testing

4.1 Test setup

The performances of the developed wireless sensor for fatigue crack detection and failure warning were examined using the data acquired from steel (SS400) welded specimens. The overall dimensions of the specimens are $360 \times 100 \times 3$ mm^3, and the details of the specimen's geometry and the packaged PZT module are described in Fig. 6(a). Two 3 mm thick plates were weld via butt welding with a double V shape. The packaged PZT module, composed of PZT_H (for HF excitation), PZT_L (for LF excitation), and PZT_S (for sensing response), were glued on each specimen. Two specimens were used for the fatigue crack detection, and three for the failure warning experiments. For the fatigue crack detection experiment, one intact specimen and the other specimen with a fatigue crack were prepared. A real fatigue crack is introduced to the damaged specimen through a cyclic loading test. The
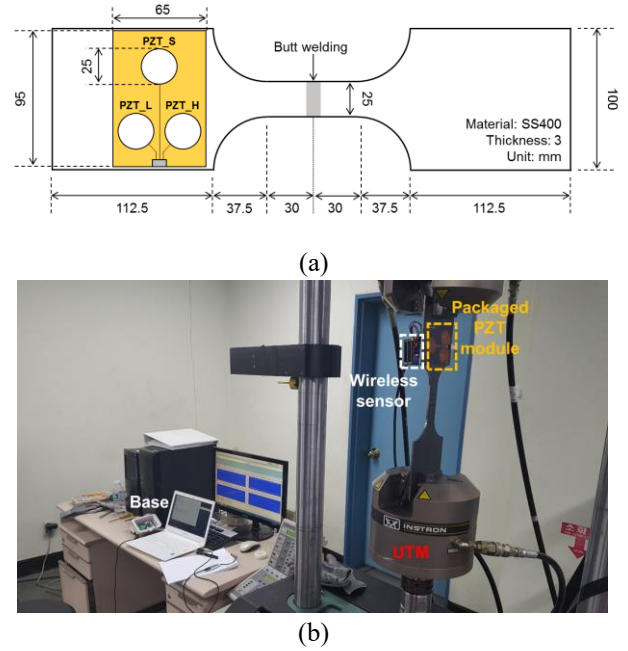

(a)

(b)

Fig. 6 Laboratory test setup for online fatigue crack detection and failure warning: (a) Description of the steel welded specimen, and (b) configuration of cyclic loading test

cyclic loading test was performed using a universal testing machine (INSTRON 8801) with a maximum load of 31 kN, a stress ratio of 0.1, and a cycle rate of 10 Hz, as shown in Fig. 6(b). About 4 mm long fatigue crack was created along the welding of the specimen after 70,000 loading cycles. For the failure warning experiment, three specimens, specimen 1 to 3, were fabricated with stress ratios of 0.2, 0.1 and 0.05, respectively. The rest of the cyclic loading test setup was identical to the previous test.

The HF and LF signals from the wireless sensor were set with a peak-to-peak voltage of 20 V, and the corresponding responses were measured with a sampling rate of 1 MHz for 0.25 seconds. To enhance the signal-to-noise ratio, the responses were averaged four times in the time domain. Twenty-two frequency combinations of the HF and LF were selected because some of the frequency combinations may not meet the binding conditions. The frequency of the HF signal was either 185 kHz or 186 kHz, and the frequency of the LF signal was varied from 40 kHz to 50 kHz with 1 kHz increment. The average nonlinear parameter and the presence of a fatigue crack were wirelessly transmitted to the base station.

4.2 Fatigue crack detection results

The NI values obtained from the intact and the damaged specimens were arranged in the ascending order, as shown in Fig. 7(a) and (b). With a 99% confidence interval, the threshold value in Eq. (1) was calculated by fitting an exponential distribution to four $n_{\omega_b\pm\omega_a,i}$ values (N is 4 here).
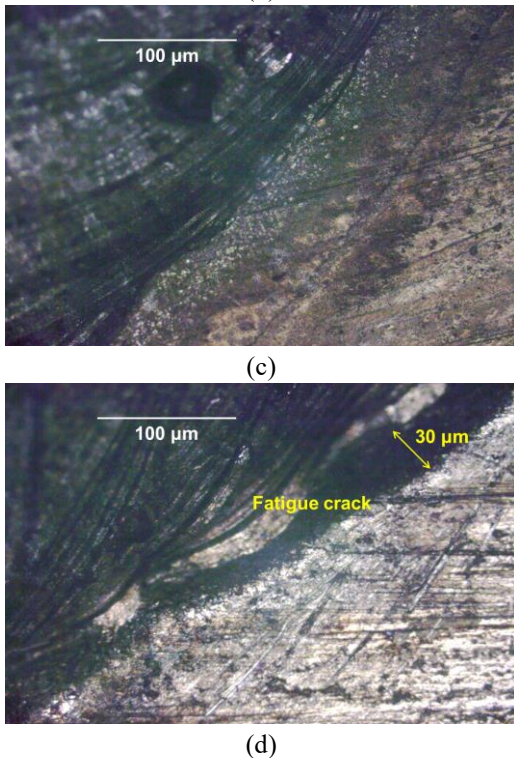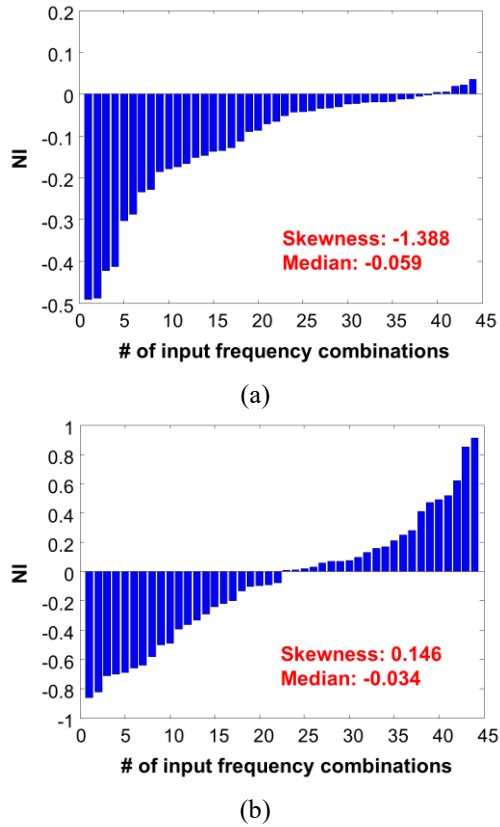
(a)

(b)

(c)

(d)

Fig. 7 Fatigue crack detection results using the wireless sensor and a microscope: (a) NI values from the intact specimen, (b) NI values from the damaged specimen, (c) microscopic image of the intact specimen, and (d) microscopic image of the damaged specimen

Because there are 22 different input frequency combinations (two choices for HF input and 11 choices for
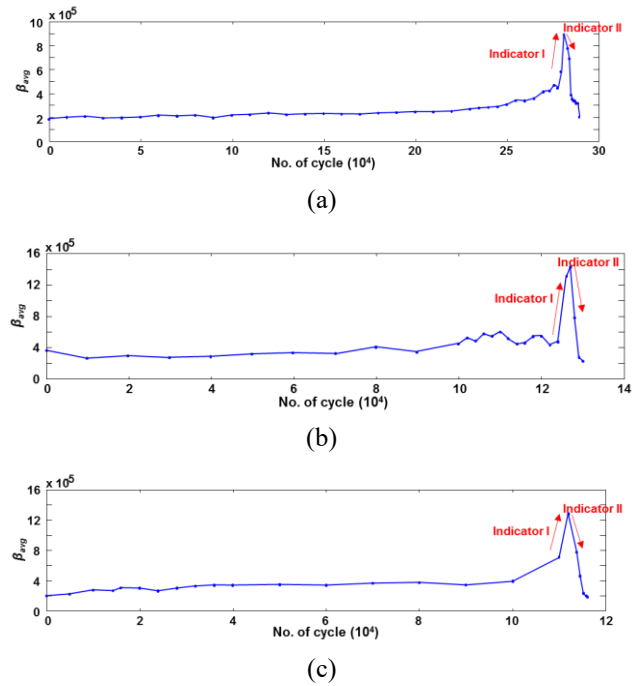

(a)

(b)

(c)

Fig. 8 Failure warning test results using the wireless sensor: the stress ratio is 0.2, 0.1, 0.05 for (a) specimen 1, (b) specimen 2, and (c) specimen 3, respectively.

LF input) and each frequency combination produces two NI values at the sum and difference of high and low frequency inputs, a total of 44 NI values were obtained. Then, the skewness and median statistics were calculated from these 44 NI values. Both the skewness and median values were below zero for the intact specimen (Fig. 7(a)), while the skewness value was positive for the damaged specimen (Fig. 7(b)).

An optical microscope captured the enlarged images of the welded parts of both intact and damaged specimens. No crack was found in the intact specimen (Fig. 7(c)), while a 4 mm long and 30 μm wide fatigue crack was found in the damaged specimen (Fig. 7(d)).

4.3 Failure warning results

The wireless sensor measured the β_{avg} values around every 10,000 loading cycles in the early stage of fatigue life, and around every 1,000 cycles near the failure point. In Fig. 8(a), (b) and (c), the β_{avg} values obtained from specimens 1, 2, and 3 were plotted with respect to loading cycles.

For specimen 1 with a stress ratio of 0.2, Indicator I appeared at 279,678 cycles, and the failure warning (Indicator II) was given at 282,885 cycles, which was 6,744 cycles before the actual failure of the specimen (289,629 cycles). For specimen 2 with a stress ratio of 0.1, Indicator I and II were observed at 126,005, and 128,006 cycles, respectively. The failure warning was provided 1,973 cycles before the actual failure (129,979 cycles). For specimen 3 with a stress ratio of 0.05, Indicator I and II occurred at 110,005 and 113,800 cycles, respectively, while the specimen 3 failed at 116,097 cycles. Therefore, the wireless

Table 1 Power consumption of the wireless sensor in different operation modes

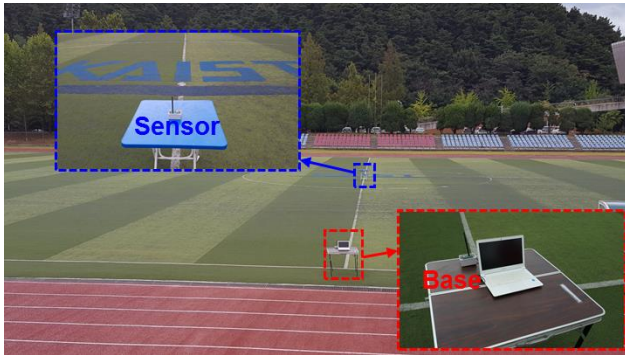| Power mode	Power consumption (mW)	Time (sec)	Energy consumption (J)
Active	748.9	163	122.06
Sleep	0.0495	1783997	88.31
Sniff	2.4	30240	72.58
Total	-	1814400 (3 weeks)	282.95

Fig. 9 Test setups for outdoor wireless communication test

sensor successfully provided failure warnings around 3,600 cycles before the failure of the specimens (that is when about 97.6% of the fatigue lives are reached).

### 4.4 Power/Energy consumption measurements

To measure the power/energy consumption of the wireless sensor, a power measurement test was performed. A digital multimeter (Keithley 2000) measured the current flowed out from the battery while the wireless sensor was in operation (attached to the steel welded specimen). All the testing parameters of the wireless sensor were identical to the aforementioned fatigue crack detection test, and the battery voltage was assumed to remain at 3.2 V during the measurement. In the periodic mode, the duty cycle of the wireless sensor was set to three weeks. Multiplying the power consumption by the time duration, the energy consumption of the wireless sensor for three weeks was estimated.

Table 1 summarizes the power/energy consumption of each operation mode of the wireless sensor. In the active mode, the packaged PZT, excitation/sensing module, data acquisition/processing module, and the wireless communication module consumed an average of 748.9 mW for 163 seconds, and the maximum peak power was around 1.2 W. In the sleep mode, the average power consumption of the wireless communication module was 49.5 μW. In the sniff mode, the wireless communication module consumed 2.4 mW during a second in every one minute. Total energy consumption of the wireless sensor for three weeks was 282.95 J.
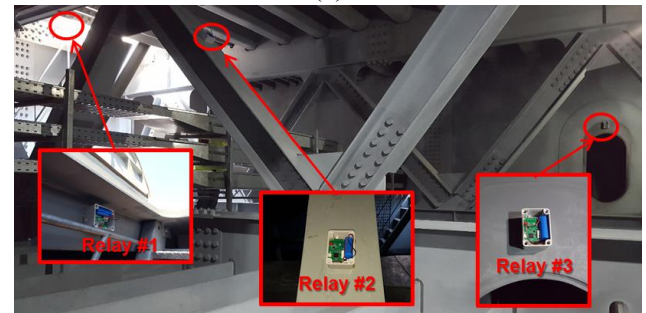
Previously, energy harvesting techniques were adopted to recharge the battery in the wireless sensor. A solar energy harvesting technique supplied abundant energy to the wireless sensors when the sensor was placed outside of Yeongjong Grand bridge (Sohn *et al.* 2016). When the

(a)
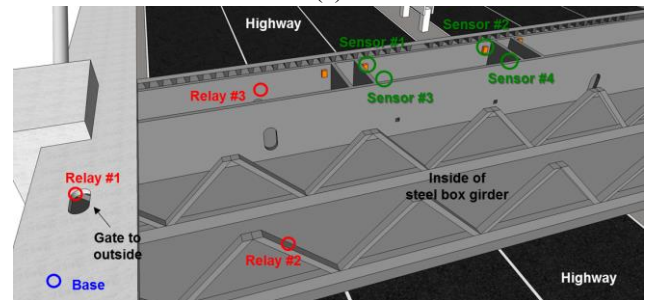
(b)

(c)

(d)

Fig. 10 Fatigue crack detection test conducted in Yeongjong Grand Bridge: (a) Perspective view of Yeongjong Grand Bridge, (b) Positions of the wireless sensors and relays installed inside the steel box girder, (c) installations of the relays, and (d) installation of sensor #1

wireless sensors were installed inside the box girders of the bridge, the solar energy harvesting was not possible and a vibration energy harvesting technique was adopted instead. The vibration energy harvesting system was able to provide around 25% of the energy required to operate the wireless sensor (Yang *et al.* 2018).

4.5 Wireless communication results

As shown in Fig. 9, a wireless communication test with a varying distance between the wireless sensor and the base was conducted in an outdoor environment to examine the reliability of wireless communication. The sensor sent data packets of 115 bytes, which is equivalent to the actual data packets (sensor identification, and the values of skewness, median, and average nonlinear parameter) sent by the wireless sensor, 1000 times at 1.2 kbps data rate. The transmitting power was set to be its maximum (14 dBm), and a 16 cm long external isotropic antenna with 3 dBi gain was installed on both the sensor and the base. The base received the data packets, and the success rate was measured by counting how many times the base receives the data packets. The location of the base was fixed, and the location of the sensor from the base was varied with 5 m increment.

When the distance between the base and the sensor was 20 m, the success rate and the receiving power were 91.6% and around -60 dBm, respectively. However, once the distance between the base and the sensor reached 25 m, the receiving power suddenly decreased below -80 dBm, and the base received the data packets with the success rate of less than 20 %.

5. Yeongjong Grand Bridge testing

5.1 Test setup

Yeongjong Grand Bridge, the world first three-dimensional (3D) self-anchored suspension bridge, connects Yeongjong Island (Incheon International Airport) to the mainland (Incheon) of South Korea (Fig. 10(a)). The bridge consists of the upper deck (six lanes for highways) and the lower deck (four lanes for highways and two lanes for railways), and the total length and the main span length of the bridge are 4420 m and 300 m, respectively. More than 390 sensors including accelerometers and GPS sensors are installed on the bridge, and New Airport Hiway Co. manages the maintenance of the bridge (Lim *et al.* 2016).

Incheon Airport Railroad Express (A'REX) has been passing Yeongjong Grand Bridge since 2007. Korean Train Express (KTX) has passed the bridge from 2014 to 2018. The weight of the A'REX train is about 210 ton, and the weight of the KTX train is about 771 ton, which is around 3.6 times heavier than the weight of the A'REX train. The operation of KTX was not initially considered during the design stage of the bridge so that New Airport Hiway Co. has concerned for fatigue damage due to the heavy weight of the KTX train. Therefore, the proposed wireless sensors for fatigue crack detection and failure warning were deployed to the bridge.

As shown in Fig. 10(b) and (c), four wireless sensors were installed near the welded parts inside the steel box girder, where high-stress concentration is expected. Based on periodic visual inspection and NDT, those welded parts are confirmed to be susceptible to fatigue cracks. Since the base was located outside the steel box girder (on the upper deck) and the wireless sensors are located in an enclosed

Table 2 Fatigue crack detection results from the wireless sensors and comparison with NDT results

Sensor number	1st measurement			2nd measurement			3rd measurement			By NDT
	Skew.	Median	Result	Skew.	Median	Result	Skew.	Median	Result	
#1	-1.712	-3.05e-2	Intact	-1.267	-5.15e-2	Intact	-1.424	-8.35e-2	Intact	Intact
#2	-1.735	-1.04e-2	Intact	-2.255	-1.89e-2	Intact	-1.525	-2.47e-2	Intact	Intact
#3	-2.136	-7.47e-2	Intact	-1.667	-5.91e-2	Intact	-1.945	-6.76e-2	Intact	Intact
#4	-1.525	-2.44e-2	Intact	-1.298	-4.04e-2	Intact	-1.107	-9.09e-2	Intact	Intact

chamber with a small opening, two relays were required. The relay delivered the wake-up signal from the base to the wireless sensors and sent back the corresponding data packets from the wireless sensors to the base. The deployments of the wireless sensors, relays, and base are shown in Fig. 10(b) and (c).

Whenever A'REX passed through the test point, the base sent the wake-up signal to relay 1. The wake-up signal was passed on to relay 3 through relay 2, and relay 3 broadcasted the wake-up signal to the wireless sensors. Then, the wireless sensors measured ultrasonic responses, determined the presence of a fatigue crack, sent out the diagnoses to the relay 3, and went back to the sleep mode. The diagnoses were transmitted to the base through relays 3, 2, and 1.

The frequency of the HF input was selected as either 186 kHz or 187 kHz, and the frequency of the LF input was varied from 40 kHz to 50 kHz with 1 kHz increment. The other test parameters were identical to the laboratory test.

5.2 Test results

The NI values were measured from the wireless sensors using a 99.99% confidence interval. To check the consistency of the fatigue crack detection performance, the same test was repeated three times. No indication of crack was given from all wireless sensors as shown in Table 2. In 2017, visual inspection and magnetic particle testing were performed on these inspection points, substantiating the diagnoses from the wireless sensors. Note that additional wireless sensors were placed in additional inspection points, and their diagnoses were also consistent with the visual inspection and magnetic particle test results. But these results are not reported here due to confidentiality. Although the distance between relay 3 and the farthest wireless sensor was over 20 m, the success rate inside the steel box girder was over 90%, which is better than the success rate of the previous outdoor experiment. It is speculated that the walls of the steel box girder served as wave guides for RF signals.

6. Conclusions

In this study, a wireless sensor based on nonlinear ultrasonic modulation measurement is developed for online monitoring of a metallic structure susceptible to a fatigue crack. The wireless sensor is composed of five major modules: the packaged PZT module, the excitation/sensing module, the data acquisition/processing module, the

wireless communication module, and the power supply module. The packaged PZT module attached to a structure and the excitation/sensing module generate ultrasonic wave at two distinctive frequencies and capture and digitize corresponding responses. The data acquisition/processing module, where the autonomous fatigue crack detection and failure warning algorithms are implemented, acquires measured responses, identifies the existence of a fatigue crack, and provides a warning for failure. The wireless communication module transmits the processed results to the base through the two-levels duty cycling MAC. Although the wireless sensor basically operates in a periodic mode with a duty cycle of three weeks, an event-driven mode is also supported initiate inspection after extreme events like earthquakes. A lithium phosphate battery with 1500 mAh capacity is used as the power supply module.

The performance and applicability of the wireless sensor were successfully validated through laboratory and field tests. In the laboratory testing, the wireless sensor detected the fatigue crack with around 30 μm overall width of the crack in the steel welded specimen and gave alarms when about 97.6% of the fatigue lives of the steel welded specimens were reached. The wireless sensor consumed 282.95 J for 3 weeks and transmitted the processed results up to 20 m away with more than 90% success rate. Furthermore, the field test conducted in Yeongjong Grand Bridge, the wireless sensors produced fatigue crack detection results which were identical to the visual inspection and the magnetic particle test results.

Although the wireless sensor is designed for low power operation, the life expectancy of the wireless sensor is around 1.5 years and periodic battery replacement is required. Also, the success rate is yet insufficient for reliable field applications. Therefore, a future study will focus on minimization of the energy consumption, integration with energy harvesting techniques and enhancing the reliability of wireless communication. Furthermore, the long-term reliability of the wireless sensors deployed on Yeongjong Grand Bridge will be investigated to replace conventional NDT and wired sensing techniques.

Acknowledgments

References

Amura, M and Meo, M. (2012), "Prediction of residual fatigue life using nonlinear ultrasound", *Smart Mater. Struct.*, **21**(4), 045001.

Caizzone, S., DiGampaolo, E. and Marrocco, G. (2014), "Wireless crack monitoring by stationary phase measurements from coupled RFID tags", *IEEE Trans. Antenn. Propagat.*, **62**(12), 6412-6419.

Cantrell, J.H. and Yost, W.T. (2001), "Nonlinear ultrasonic characterization of fatigue microstructures", *Int. J. Fatig.*, **23**, 487-490.

Chan, T.H., Li, Z. and Ko, J.M. (2004), "Evaluation of typhoon induced fatigue damage using health monitoring data for the Tsing Ma Bridge", *Struct. Eng. Mech.*, **17**(5), 655-670.

Chen, H.L.R. and Choi, J.H. (2006), "Fatigue crack growth and remaining life estimation of AVLB components", *Struct. Eng. Mech.*, **23**(6), 651-674.

Chen, J., Yuan, S., Qiu L., Cai, J. and Yang, W. (2016), "Research on a lamb wave and particle filter-based on-line crack propagation prognosis method", *Sens.*, **16**(3), 320.

Chintalapudi, K., Fu, T., Paek, J., Kothari, N., Rangwala, S., Cafferey, J. and Masri, S. (2006), "Monitoring civil structures with a wireless sensor network", *IEEE Intern. Comput.*, **10**(2), 26-34.

De Lima, W. and Hamilton, M. (2003), "Finite-amplitude waves in isotropic elastic plates", *J. Sound Vibr.*, **265**(4), 819-839.

Duffour, P., Morbidini, M. and Cawley, P. (2006), "A study of the vibro-acoustic modulation technique for the detection of cracks in metals", *J. Acoust. Soc. Am.*, **119**(3), 1463-1475.

Fierro, G.P.M. and Meo, M. (2015), "Residual fatigue life estimation using a nonlinear ultrasound modulation method", *Smart Mater. Struct.*, **24**(2), 025040.

Forrest, P.G. (2013), *Fatigue of Metals*, Elsevier.

Gholizadeh, S., Leman, Z. and Baharudin, B. (2015), "A review of the application of acoustic emission technique in engineering", *Struct. Eng. Mech.*, **54**(6), 1075.

Grosse, C.U., Glaser, S.D. and Knuger, M. (2010), "Initial development of wireless acoustic emission sensor Motes for civil infrastructure state monitoring", *Smart Struct. Syst.*, **6**(3), 197-209.

Hamia, R., Cordier, C. and Dolabdjian, C. (2014), "Eddy-current non-destructive testing system for the determination of crack orientation", *Ndt E Int.*, **61**, 24-28.

Ihn, J.B. and Chang, F.K. (2004), "Detection and monitoring of hidden fatigue crack growth using a built-in piezoelectric sensor/actuator network: I. Diagnostics", *Smart Mater. Struct.*, **13**(3), 609.

Jang, S., Jo, H., Cho, S., Mechitov, K., Rice, J.A., Sim, S.H. and Agha, G. (2010), "Structural health monitoring of a cable-stayed bridge using smart sensor technology: Deployment and evaluation", *Smart Struct. Syst.*, **6**(5-6), 461-480.

Jhang, K.Y. (2009), "Nonlinear ultrasonic techniques for nondestructive assessment of micro damage in material: a review", *Int. J. Prec. Eng. Manufact.*, **10**(1), 123-135.

Kilic, G. (2014), "Wireless sensor network protocol comparison for bridge health assessment", *Structu. Eng. Mech.*, **49**(4), 509-521.

Kim, Y., Lim, H.J. and Sohn, H. (2018), "Nonlinear ultrasonic modulation based failure warning for aluminum plates subject to fatigue loading", *Int. J. Fatig.*, **114**, 130-137.

Knopp, J.S., Aldrin, J.C. and Jata, K.V. (2009), "Computational methods in eddy current crack detection at fastener sites in multi-layer structures", *Nondestruct. Test. Evaluat.*, **24**(1-2), 103-120.

Kwon, S.D., Park, J. and Law, K. (2013), "Electromagnetic energy harvester with repulsively stacked multilayer magnets for low frequency vibrations", *Smart Mater. Struct.*, **22**(5), 055007.

Li, N., Sun, J., Jiao, J., Wu, B. and He, C. (2016), "Quantitative evaluation of micro-cracks using nonlinear ultrasonic modulation method", *Ndt E Int.*, **79**, 63-72.

Lim, H.J., Kim, Y., Koo, G., Yang, S., Sohn, H., Bae, I.H. and

Jang, J.H. (2016), "Development and field application of a nonlinear ultrasonic modulation technique for fatigue crack detection without reference data from an intact condition", *Smart Mater. Struct.*, **25**(9), 095055.

Lim, H.J., Sohn, H. and Liu, P. (2014), "Binding conditions for nonlinear ultrasonic generation unifying wave propagation and vibration", *Appl. Phys. Lett.*, **104**(21), 214103.

Liu, P., Lim, H.J., Yang, S., Sohn, H., Lee, C.H., Yi, Y. and Bae, I.H. (2017), "Development of a "stick-and-detect" wireless sensor node for fatigue crack detection", *Structural Health Monitor.*, **16**(2), 153-163.

Liu, Y., He, C., Huang, C., Khan, M.K. and Wang, Q. (2014), "Very long life fatigue behaviors of 16Mn steel and welded joint", *Struct. Eng. Mech.*, **52**(5), 889-901.

Lynch, J.P., Law, K.H., Kiremidjian, A.S., Carryer, E., Farrar, C.R., Sohn, H. and Wait, J.R. (2004), "Design and performance validation of a wireless sensing unit for structural monitoring applications", *Struct. Eng. Mech.*, **17**(3-4), 393-408.

Lynch, J.P., Wang, Y., Loh, K.J., Yi, J.H. and Yun, C.B. (2006), "Performance monitoring of the Geumdang Bridge using a dense network of high-resolution wireless sensos", *Smart Mater. Struct.*, **15**(6), 1561.

Mainwaring, A., Culler, D., Polastre, J., Szewczyk, R. and Anderson, J. (2002), "Wireless sensor networks for habitat monitoring", *Proceedings of the 1st ACM International Workshop on Wireless Sensor Networks and Applications*, Atlanta, Georgia, U.S.A., September.

Marin, A., Kishore, R., Schaab, D.A., Vuckovic, D. and Priya, S. 2016), "Micro wind turbine for powering wireless sensor nodes", *Energy Harvest. Syst.*, **3**(2), 139-152.

McCullagh J, Galchev T, Peterson R, *et al.* (2014), "Long-term testing of a vibration harvesting system for the structural health monitoring of bridges", *Sens. Actuat. A: Phys.*, **217**, 139-150.

Mi, B., Michaels, J.E. and Michaels, T.E. (2006), "An ultrasonic method for dynamic monitoring of fatigue crack initiation and growth", *J. Acoust. Soc. Am.*, **119**(1), 74-85.

Mix, P.E. (2005), *Introduction to Nondestructive Testing: A Training Guide*, John Wiley & Sons.

Nair, A. and Cai, C. (2010), "Acoustic emission monitoring of bridges: Review and case studies", *Eng. Struct.*, **32**(6), 1704-1714.

Nallasivam, K., Talukdar, S. and Dutta, A. (2008), "Fatigue life prediction of horizontally curved thin walled box girder steel bridges", *Struct. Eng. Mech.*, **28**(4), 387-410.

Rabiei, M. and Modarres, M. (2013), "Quantitative methods for structural health management using in situ acoustic emission monitoring", *Int. J. Fatig.*, **49**, 81-89.

Roberts, T. and Talebzadeh, M. (2003), "Acoustic emission monitoring of fatigue crack propagation", *J. Constr. Steel Res.*, **59**(6), 695-712.

Rokhlin, S. and Kim, J.Y. (2003), "In situ ultrasonic monitoring of surface fatigue crack initiation and growth from surface cavity", *Int. J. Fatig.*, **25**(1), 41-49.

Ruiz-Cárcel, C., Hernani-Ros, E., Cao, Y. and Mba, D. (2014), "Use of spectral kurtosis for improving signal to noise ratio of acoustic emission signal from defective bearings", *J. Fail. Analy. Prevent.*, **14**(3), 363-371.

Sankararaman, S., Ling, Y. and Mahadevan, S. (2011), "Uncertainty quantification and model validation of fatigue crack growth prediction", *Eng. Fract. Mech.*, **78**, 1487-1504.

Sazonov, E., Krishnamurthy, V. and Schilling, R. (2010), "Wireless intelligent sensor and actuator network-a scalable platform for time-synchronous applications of structural health monitoring", *Struct. Health Monitor.*, **9**, 465-476.

Sohn, H., Lim, H.J., DeSimio, M.P., Brown, K. and Derriso, M. (2014), "Nonlinear ultrasonic wave modulation for online fatigue crack detection", *J. Sound Vibr.*, **333**(5), 1473-1484.

Sohn, H., Lim, H.J., Kim, J.M., *et al.* (2016), "Self-sufficient and self-contained sensing for local monitoring of in-situ bridge structures", *Proceedings of the 8th European Workshop on Structural Health Monitoring*, Bilbao, Spain, July.

Su, Z., Zhou, C., Hong, M., Cheng, L., Wang, Q. and Qing, X. (2014), "Acousto-ultrasonics-based fatigue damage characterization: Linear versus nonlinear signal features", *Mech. Syst. Sign. Proc.*, **45**(1), 225-239.

Sunny, A.I., Tian, G.Y., Zhang, J. and Pal, M. (2016), "Low frequency (LF) RFID sensors and selective transient feature extraction for corrosion characterization", *Sens. Actuat. A: Phys.*, **241**, 34-43.

Tanner, N.A., Wait, J.R., Farrar, C.R. and Sohn, H. (2003), "Structural health monitoring using modular wireless sensors", *J. Intellig. Mater. Syst. Struct.*, **14**(1), 43-56.

Van Den Abeele, K.A., Johnson, P.A. and Sutin, A. (2000), "Nonlinear elastic wave spectroscopy (NEWS) techniques to discern material damage, part I: Nonlinear wave modulation spectroscopy (NWMS)", *J. Res. Nondestruct. Evaluat.*, **12**(1), 17-30.

Wijetunge, S., Gunawardana, U. and Liyanapathirana, R. (2010), "Wireless sensor networks for structural health monitoring: Considerations for communication protocol design", *Proceedings of the 2010 IEEE 17th International Conference on IEEE*, Doha, Qatar, April.

Wu, W. and Ni, C. (2004), "Probabilistic models of fatigue crack propagation and their experimental verification", *Probabilist. Eng. Mech.*, **19**(3), 247-257.

Yang, S., Jung, S.Y., Kim, K., Liu, P., Lee, S., Kim, J. and Sohn, H. (2018), "Development of a tunable low-frequency vibration energy harvester and its application to a self-contained wireless fatigue crack detection sensor", *Struct. Health Monitor.*, 1475921718786886.

Zaitsev, V.Y., Nazarov, V.E. and Talanov, V.I. (2006), "Nonclassical'manifestations of microstructure-induced nonlinearities: New prospects for acoustic diagnostics", *Phys.-Uspekhi*, **49**(1), 89-94.

Zhang, J. and Tian, G.Y. (2016), "UHF RFID tag antenna-based sensing for corrosion detection & characterization using principal component analysis", *IEEE Trans. Antenn. Propagat.*, **64**(10), 4405-4414.

Zilberstein, V., Schlicker, D., Walrath, K., Weiss, V. and Goldfine, N. (2001), "MWM eddy current sensors for monitoring of crack initiation and growth during fatigue tests and in service", *Int. J. Fatig.*, **23**, 477-485.

CC